Combined photoluminescence-imaging and deep-level transient spectroscopy of recombination processes at stacking faults in 4*H*-SiC

A. Galeckas,* A. Hallén, S. Majdi, and J. Linnros
Department of Microelectronics and Applied Physics, Royal Institute of Technology, Electrum 229, SE-164 40 Stockholm, Sweden

P. Pirouz
Department of Materials Science and Engineering, Case Western Reserve University, Cleveland, Ohio 44106-7204, USA
(Received 20 October 2006; published 14 December 2006)

We report on electronic properties of single- and double-layer stacking faults in 4*H*-SiC and provide an insight into apparent distinctions of recombination-enhanced defect reactions at these faults. Photoluminescence imaging spectroscopy and deep-level transient spectroscopy experiments reveal key constituents of radiative recombination and also provide firm evidence of nonradiative centers at $E_V+0.38$ eV responsible for recombination-enhanced mobility of silicon-core partial dislocations. A comprehensive energy level model is proposed allowing for a qualitative description of recombination activity at different types of stacking faults and the corresponding bounding partial dislocations.

DOI: 10.1103/PhysRevB.74.233203 PACS number(s): 61.72.Ff, 81.05.Hd, 81.70.Fy, 85.30.Kk

Structural instability issues still hamper full-scale commercialization of hexagonal SiC material for high-power bipolar electronics despite substantial progress in understanding (for a review, see Ref. 1) and handling of this problem.[2,3] Studies show that degradation in the active region of forward operating devices is caused by spontaneous formation of planar defects,[4,5] identified as basal plane stacking faults (SF) bounded by Shockley partial dislocations (PD).[6,7] The phenomenon of recombination enhanced dislocation glide (REDG),[5,8] also known as the "phonon-kick" mechanism,[9,10] is believed to be responsible for the lateral expansion of SFs. Part of the electron-hole (*e-h*) recombination energy is redirected into nonradiative sites along the dislocation line to aid formation and migration of kinks, thus dramatically reducing the activation barrier for glide.[8,10] Apart from this strong REDG effect, theoretical models interpret an SF in 4*H*-SiC as a two-dimensional (2D) quantum well (QW) for the conduction band electrons.[11,12] Since entrapment of electrons in the QWs leads to reduction of the mean electronic energy, a faulted *n*-type crystal is supposed to be more stable than a perfect one. Indeed, the spontaneous formation of SFs reported in highly *n*-doped 4*H*-SiC (Ref. 13) apparently supports this assumption. It appears, however, that structure and mobility properties of the faults formed by the doping effect differ from those generated in operating devices by the REDG mechanism, thus fueling discussions about the actual driving force for SF formation.[14–16] In particular, the issues which call for clarification are why exclusively single-layer stacking faults (1SF) form in the degrading devices, whereas double-layer faults (2SF) occur in highly *n*-doped material, and also why 2SFs remain stationary while 1SFs expand in presence of the *e-h* plasma.

In this paper, we address these differences of single and double stacking faults and provide an insight into the details of recombination-enhanced defect reactions in 4*H*-SiC.

A common way to study recombination activity of dislocations is by some kind of scanning technique, e.g., cathodoluminescence (CL),[7] photoluminescence (PL),[4] or electron-beam induced current (EBIC).[17] An alternative approach, allowing for instantaneous mapping of extended defects and also monitoring of structural instabilities, relies on electroluminescence imaging and hence is applicable only to forward operating devices.[18] In the present work, an all-optical method of imaging spectroscopy is used to study dynamics and luminescence properties of basal plane SFs both within devices and in virginal epitaxial layers. A series of ns-duration pulses from a tunable wavelength Nd-YAG OPO laser is used to generate excess *e-h* pairs and, consequently, to trigger recombination-enhanced motion of dislocations. The motion is probed *in situ* by time-lapse imaging of the background PL, set off by low intensity excitation from a 325 nm cw-HeCd laser. This pump-and-probe approach is implemented into a time-resolved imaging spectroscopy setup (see Ref. 19 for more detail) to examine several 4*H*-SiC homoepitaxial n^-/n^+ structures and fully processed $p^+/n^-/n^+$ diodes.[20] In both cases, the $\sim$40 μm-thick nominally undoped $n^- \sim 5\times10^{14}$ cm^{-3} epilayers were grown by CVD on $n^+ \sim 10^{19}$ cm^{-3} substrates from Cree, Inc. A schematic of the experiment and typical examples of plan-view and cross-sectional PL imaging are given in Fig. 1. An adaptable optical filtration, i.e. imaging of PL in a narrow spectral range, was employed to visualize luminescent defects, otherwise indistinguishable against dominant background of intrinsic band-edge and deep-level luminescence. In spectral analysis, similar low contrast issues were resolved by utilizing spatially-resolved differential PL, which greatly enhances selectivity for emission from the extended defects. In view of the fact that PL peaks merely indicate energy separation between the levels involved in radiative transition and not the actual position in the band gap, a complementary scan of electrically active states has been carried out by deep-level-transient spectrometry (DLTS). A highly degraded $p^+/n^-/n^+$ diode with a SF density in excess of 10^3 cm^{-1} was selected for DLTS experiments.

To get further insight into radiative and nonradiative recombination processes at stacking faults in 4*H*-SiC we compare PL and REDG characteristics of optically-induced and in-grown SFs found within the same homoepitaxial structure

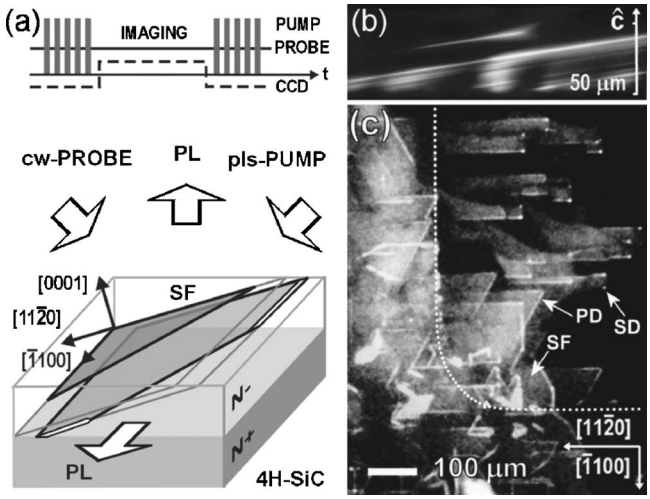

FIG. 1. (a) Schematic and time line of a *pump-probe* PL imaging experiment: structural instabilities are *probed* by a time-gated CCD after exposure to a series of intense *pump* pulses. (b) Cross-sectional and (c) plan-view PL micrographs (overlay of two monochromatic 430 nm and 750 nm patterns), exposing threading type dislocations (TD) as well as basal plane stacking faults (SF) bounded by partial dislocations (PD); dotted line marks the border between virginal n^-/n^+ and processed $p^+/n^-/n^+$ areas (half of a diode in the upper-right area).

[see Figs. 2(a) and 2(b)]. The principal radiative channels are evident from the differential PL spectra plotted in Fig. 3. The stacking faults demonstrate characteristic peaks associated with $E_C-0.3$ eV and $E_C-0.6$ eV split-off levels, which are consistent with first principles calculations for 1SF and 2SF related quantum wells.[11,12] It is interesting to note that partial dislocations bordering 1SF and 2SF type faults exhibit clearly dissimilar spectral signatures corresponding to optical transitions of about 1.6 eV and 1.9 eV, respectively. Our experiments show that unlike the single-layer 1SFs, which expand under illumination, the in-grown 2SFs remain immobile up to excitations causing structural damage of SiC material. Furthermore, we find that besides the well-established luminescence of the mobile Si(g) edges, a weak emission from the fixed C(g) edges also takes place, as can be seen in Fig. 2(a). The yield differs by more than an order

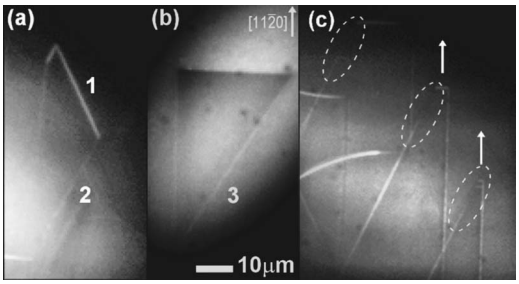

FIG. 2. PL micrographs of partial dislocations bordering (a) single (1SF) and (b) in-grown double stacking fault (2SF). Spatially-resolved spectra were collected from the mobile leading (1) and stationary trailing (2) edges of the 1SF and also from the PDs (3) surrounding 2SF. (c) Regions of quenched luminescence following after the gliding segments of the expanding SFs.

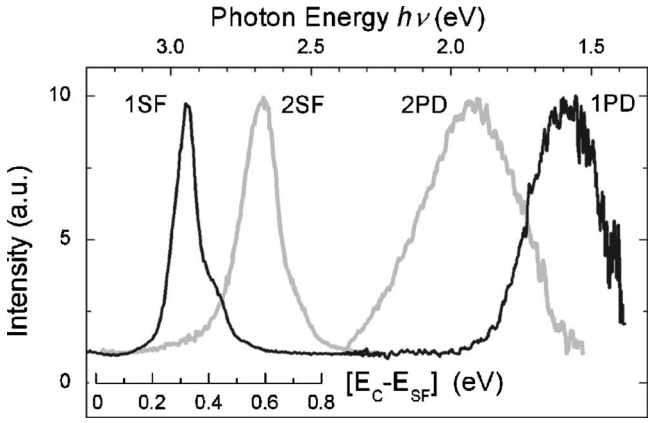

FIG. 3. Spectral signatures (normalized differential PL at 300 K) of single- (1SF) and double-layer (2SF) stacking faults and corresponding bounding partial dislocations, labeled 1PD and 2PD, respectively.

of magnitude, as indicated by the PL contrast ratio of the corresponding segments, i.e., $[I_{Si(g)}-I_0]/[I_{C(g)}-I_0]>10$, where I_0 is the background intensity. More importantly, the luminescence spectra obtained separately from the gliding and the stationary partials appear fairly similar, the latter exhibiting slightly broader high-energy shoulder. This spectral similarity is somewhat unexpected, bearing in mind that the gliding and stationary PD segments at the edges of the SF are believed to have different core natures, silicon Si(g) and carbon C(g), respectively.[1] Although the onset of passive scattering of light originated from the mobile Si(g) partials cannot be ruled out, the results can best be explained assuming different density of otherwise identical radiative centers along Si(g) and C(g) partials. As a final point, in Fig. 2(c) we highlight clear dominance of the nonradiative processes over radiative recombination at the expanding SF. A closer inspection of optically-stimulated REDG images shows that the moving partials are always trailed by a region of quenched PL, suggesting that within the diffusion length of a PD the electrons confined in a 2D QW are primarily drained via nonradiative REDG channel.

The energy of a deep nonradiative center supporting dislocation glide, though directly not detectable in PL measurements, yet can be deduced indirectly from the difference of activation energy of dislocation glide under illumination [~0.25 eV (Ref. 5)] and in the dark [~2.5 eV (Ref. 21)], suggesting an approximate value of 2.25 eV. Recent below-gap excitation-spectrometry experiments provide fairly similar ~2.4 eV threshold energy for REDG activation.[15] A direct method for determining position of the energy states is by using DLTS, however, until now this technique failed to reveal additional carrier traps associated with structural degradation, most likely because of too low dislocation content. As an argument, in Fig. 4 we present measurement results of an extremely degraded $p^+/n^-/n^+$ diode, exhibiting two distinct DLTS peaks. While the smaller positive peak at around 280 K corresponds to a well-known $Z1/Z2$ defect frequently observed in as-grown 4H-SiC,[22] the larger negative peak at around 140 K, to the best of our knowledge, has not previously been reported and is only seen in highly degraded

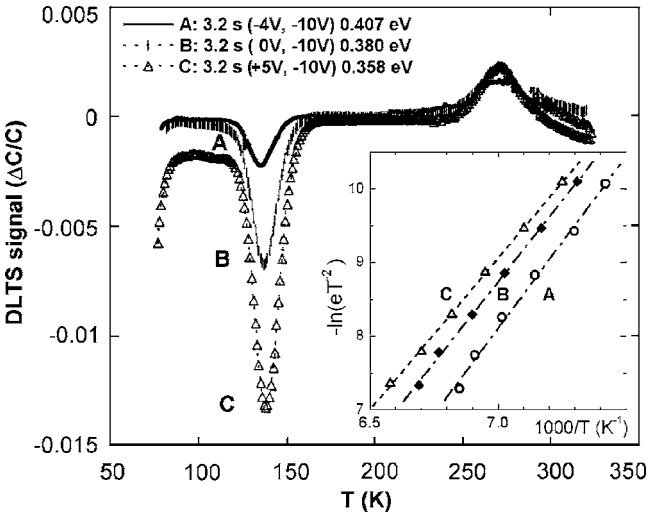

FIG. 4. DLTS spectra of a highly degraded $p^+/n^-/n^+$ diode, showing the $Z1/Z2$ level and a new minority carrier (hole) trap. The spectra were recorded with a rate window of 3.2 s, reverse bias of −10 V and filling pulse amplitudes of −4 V, 0 V, and +5 V for curves *A*, *B*, and *C*, respectively. Note that the filling pulse bias has no effect on the $Z1/Z2$ peaks. The inset shows Arrhenius plots for the hole trap, yielding slightly different values for curves *A*, *B*, and *C* due to doping compensation.

samples. The energy position of this newly emerged hole trap is estimated by a standard T^2 correction at $E_T=E_V+0.38\pm0.2$ eV. In view of the fact that the magnitude of DLTS peak increases strongly with forward bias without showing any sign of saturation, the amount of injected holes is apparently insufficient to fill all traps, and consequently their concentration can only be approximated. The largest peak in Fig. 4 (curve *C*) corresponds to a concentration of about 5×10^{13} cm^{-3}, which should be considered as a lower limit. The detected new trap level appears closely matched by first-principle calculations, which predict electrical activity only for Si(g) type partial associated with a deep $E_V+0.4$ eV state in the band gap.[23] In the presence of an excess concentration of electron-hole pairs, part of the recombination energy is released nonradiatively via these traps to aid formation and migration of kinks, thus reducing the activation barrier for dislocation glide.

The new deep level that is revealed by DLTS cannot explain on its own the characteristic reddish luminescence of the partials bounding the stacking faults. Thus, by introducing a single radiative center positioned at $E_R\sim2$ eV above the valence-band edge, we propose a model which readily explains the observed differences in PL spectra of the partials bordering single and double-layer SFs. Figure 5 presents a collective energy level diagram of recombination activity at 1SF and 2SF type faults, which accounts for concomitant radiative and nonradiative processes at mobile Shockley partials as well as for radiative centers along stationary PDs bounding the in-grown SFs. The small valence-band discontinuity and phonon interaction do not notably change the model and are ignored for simplicity. As can be seen in the diagram, the characteristic PL of the PDs bounding 1SF and 2SF type faults then correspond to, respectively, optical transitions from the radiative center directly to the valence band ($h\nu_{2PD}=E_R\sim1.9$ eV) and from E_R to the hole-trap E_T introduced by the Si(g) partial ($h\nu_{1PD}=E_R-E_T\sim1.6$ eV). In contrast to electrically active and therefore highly mobile Si(g) partials, no midgap levels are introduced by the partials bounding the in-grown 2SFs, resulting both in blueshifted optical signature (towards 1.9 eV) and absence of REDG effect.

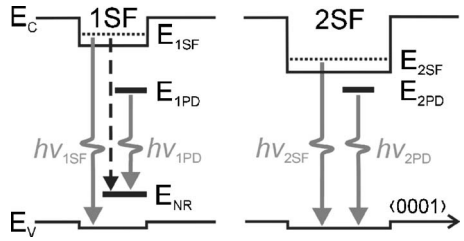

FIG. 5. Schematic of the bandgap arrangement of 4H-SiC containing 2D quantum-wells formed by 1SF and 2SF in ⟨0001⟩ direction and enclosed by PDs lying along ⟨11-20⟩. Nonradiative process aiding REDG is marked by a broken arrow; solid arrows indicate radiative transitions.

It is reasonable to assume that luminescence sources on Si(g) and C(g) partials that have basically similar characteristics originate from some common intrinsic defect, such as Si vacancy (V_{Si}) trapped at the dislocation cores. Indeed, lateral expansion of SFs under intense optical excitation appears on microscopic scale as a highly sporadic process of kink formation and migration along dislocation lines. Not surprisingly, this might be accompanied by a random occurrence of reconstruction defects, antiphase defects[24] or solitons,[25] which are associated with dangling bonds on the gliding partials (and a Si vacancy can be considered as a center of *C* dangling bonds). In fact, the discrete structure of luminescent centers along dislocation lines can be resolved on PL micrographs taken at very low excitations, revealing separate spots ~0.5 μm in diameter (apparently the diffraction-limited size) with an average linear density in excess of 10^4 cm^{-1}.

It is interesting to note that the above assumptions appear consistent with the 1.31 eV ionization energy of a negatively-charged silicon vacancy in 4*H*-SiC,[26] which is equivalent to an energy position of ~2 eV above the valence band edge (E_g-1.31~2 eV). Since negatively charged V_{Si} provides an attractive potential for valence band holes and already contains trapped electrons, it performs as a potent radiative recombination center. The likely relation of the radiative centers with charged intrinsic defects is further supported by experimental observations of apparent annealing of luminescent defects at the relatively low temperature of ~400 K (unpublished; similar effect is recently reported in Ref. 27). This moderate thermal treatment appears sufficient to seemingly eliminate (anneal out) the preexisting network of dislocations, however, luminescent dislocations re-appear again in the presence of a sufficient concentration of excess carriers, presumably as soon as the defect's charge state is restored. Indeed, thermal reexcitation of electrons trapped on the radiative sites up into the SF quantum wells seems highly feasible in view of the relatively small activation energy

($E_{1SF}-E_R \sim 1$ eV), whereas alteration of the charge state has a direct impact on the V_{Si} attractive potential for holes and consequently on its performance as a recombination center.

In summary, we provide experimental evidence of key constituents of recombination-enhanced defect reactions and present a model that allows qualitative description of this phenomenon for different types of stacking faults in 4*H*-SiC. We note, though, that interpretation of the origin of radiative midgap levels is still speculative and should be considered as a subject for further investigations. In this respect, near-field optical microscopy seems most reasonable approach for a deeper insight of radiative centers along dislocations.

This work was financially supported by the Swedish Research Council (V.R.).

*Author to whom correspondence should be sent. Electronic address: galeckas@imit.kth.se

[1] M. Skowronski and S. Ha, J. Appl. Phys. **99**, 011101 (2006).
[2] D. Nakamura, I. Gunjishima, S. Yamaguchi, T. Ito, A. Okamoto, H. Kondo, S. Onda, K. Takatori, Nature (London) **430**, 1009 (2004).
[3] J. J. Sumakeris, J. R. Jenny, and A. R. Powell, MRS Bull. **30**, 280 (2005).
[4] J. P. Bergman, H. Lendenmann, P. Å. Nilsson, U. Lindefelt, and P. Skytt, Mater. Sci. Forum **353**, 299 (2001).
[5] A. Galeckas, J. Linnros, and P. Pirouz, Appl. Phys. Lett. **81**, 883 (2002).
[6] J. Q. Liu, M. Skowronski, C. Hallin, R. Söderholm, and H. Lendenmann, Appl. Phys. Lett. **80**, 749 (2002).
[7] P. O. Persson, L. Hultman, H. Jacobson, J. P. Bergman, E. Janzén, J. M. Molina-Aldareguia, W. J. Clegg, and T. Tuomi, Appl. Phys. Lett. **80**, 4852 (2002).
[8] P. Pirouz, M. Zhang, A. Galeckas, and J. Linnros, Mater. Res. Soc. Symp. Proc. **815**, 91 (2004).
[9] J. D. Weeks, J. C. Tully, and L. C. Kimerling, Phys. Rev. B **12**, 3286 (1975).
[10] K. Maeda and S. Takeuchi, in *Dislocation in Solids*, Vol. 10, edited by F. R. N. Nabarro and M. S. Duesbery (North-Holland Publishing Company, Amsterdam, 1996), pp. 443–504.
[11] M. S. Miao, S. Limpijumnong, and W. R. L. Lambrecht, Appl. Phys. Lett. **79**, 4360 (2001).
[12] H. Iwata, U. Lindefelt, S. Öberg, and P. R. Briddon, Phys. Rev. B **65**, 033203 (2002).
[13] L. J. Brillson, S. Tumakha, R. S. Okojie, M. Zhang, and P. Pirouz, J. Phys.: Condens. Matter **16**, S1733 (2004).
[14] S. Ha, M. Skowronski, J. J. Sumakeris, M. J. Paisley, and M. K. Das, Phys. Rev. Lett. **92**, 175504 (2004).
[15] A. Galeckas, J. Linnros, and P. Pirouz, Phys. Rev. Lett. **96**, 025502 (2006).
[16] W. R. L. Lambrecht and M. S. Miao, Phys. Rev. B **73**, 155312 (2006).
[17] S. Maximenko, T. Sudarshan, and P. Pirouz, Appl. Phys. Lett. **87**, 033503 (2005).
[18] A. O. Konstantinov and H. Bleichner, Appl. Phys. Lett. **71**, 3700 (1997).
[19] A. Galeckas, J. Linnros, and M. Lindstedt, Mater. Sci. Eng., B **102**, 304 (2003).
[20] K. Rottner, A. Schöner, M. Frischholz, J.-O. Svedberg, U. Gustafsson, A. Ellison, E. Janzén, and O. Kordina, in Abstracts of ICSCIII-N'97 (Stockholm, Sweden, 1997), p. 136.
[21] P. Pirouz, M. Zhang, J.-L. Demenet, and H. M. Hobgood, J. Appl. Phys. **93**, 3279 (2003).
[22] T. A. G. Eberlein, R. Jones, and P. R. Briddon, Phys. Rev. Lett. **90**, 225502 (2003).
[23] A. T. Blumenau, C. J. Fall, R. Jones, S. Öberg, T. Frauenheim, and P. R. Briddon, Phys. Rev. B **68**, 174108 (2003).
[24] P. B. Hirsch, J. Microsc. **118**, 3 (1980).
[25] M. Heggie and R. Jones, Philos. Mag. B **48**, 365 (1983).
[26] F. Bechstedt, J. Furthmüller, U. Grossner, and C. Raffy, in *Silicon Carbide: Recent Major Advances*, edited by W. J. Choyke, H. Matsunami and G. Pensl (Springer-Verlag, Berlin, 2004), pp. 3–25.
[27] T. Miyanagi, H. Tsuchida, I. Kamata, T. Nakamura, K. Nakayama, R. Ishii and Y. Sugawara, Appl. Phys. Lett. **89**, 062104 (2006).